JPPIPA 8(5) (2022)

Jurnal Penelitian Pendidikan IPA

Journal of Research in Science Education

http://jppipa.unram.ac.id/index.php/jppipa/index

Design of PCF-SPR for Early Detection of Skin Cancer Infected Cells

Dedi Irawan[1*], Khaikal Ramadhan[2], Azhar[1]

[1]Department of Physics PMIPA, FKIP, Universitas Riau Pekanbaru, Indonesia
[2]Department of Physics, FMIPA, Institut Teknologi Bandung, Bandung, Indonesia

Received: August 25, 2022
Revised: November 16, 2022
Accepted: November 27, 2022
Published: November 30, 2022

Corresponding Author:
Dedi Irawan
dedi.irawan@lecturer.unri.ac.id

DOI: 10.29303/jppipa.v8i5.2120

Abstract: In this work, we carried out a numerical investigation of the PCF-SPR biosensor for the early detection of infected skin cancer cells and healthy cells. The study was conducted using the COMSOL Multiphysics-based FEM method. The dielectric material used in this PCF design is fused silica, while the plasmonic material is gold. The study was conducted to test the effect of the thickness of the plasmonic layer and the size of the air hole diameter on the PCF-SPR. It was found that the larger the diameter of the air hole in the proposed sensor gives a smaller confinement loss value, while the thicker the plasmonic material used also gives a small confinement loss value. The proposed PCF-SPR has a wavelength sensitivity in detecting skin cancer-infected cells of 7000 nm/RIU. These results indicate that the proposed sensor has a good performance in detecting cells infected with skin cancer.

Keywords: PCF-SPR biosensor; Skin cancer detection; Numerical investigation; High-performance

Introduction

Optical components continue to be of interest to many industries and researchers to be used as sensor components in the fields of medical, defense and security, food security, agriculture, aircraft industry, and sensing in disaster. optical components utilize light to transmit information so that they work in the wavelength domain, some of the optical components have been sold commercially and some are still undergoing development (Irawan D, 2014) Some optical components that are often used as sensors are SMF optical fiber (Saktioto et al., 2021b; Irawan, Azhar, et al., 2022; Ramadhan & Saktioto, 2021), Multi-mode fiber (MMF), Fiber Bragg Grating (FBG) (Saktioto et al., 2021a) and photonic crystal fibers (Irawan et al., 2022a; Irawan et al., 2022b), (Ramadhan, 2020). Photonic crystal fiber technology combined with the phenomenon of surface plasmon resonance continues to experience significant developments in the sensor world. PCF-SPR advantages such as wide detection range, ultra-sensitivity (Ramola et al., 2021), high birefringence (Dash & Jha, 2016), simple structure, and label-less sensing (Irawan et al., 2022).

The current research trend in developing PCF-SPR is to find PCF-SPR sensor components that have a simple geometric structure and choose dielectric and plasmonic materials that have high performance, high sensitivity, and a wide detection range. PCF-SPR has air holes around the core and cladding, air holes will cause confinement loss in sensor components. This event is also utilized in sensing temperature, magnetic field, refractive index, strain, and detecting cancer cells (Yasli, 2021; (Rahman et al., 2021). Several researchers have reported PCF-SPR geometric structures that have d-shaped, hexagonal (Rahman et al., 2021), ring-fiber, octagonal (Abdullah-Al-Shafi & Sen, 2020), and twin-core (Mollah et al., 2020). PCF-SPR also has a layer of plasmonic material to bring up the phenomenon of electron oscillations, electron oscillation events are very sensitive to environmental changes. Some of the plasmonic materials that can be used in PCF-SPR are gold, silver, copper, titanium oxide, etc. Each of these plasmonic materials has its own advantages and

How to Cite:
Irawan, D., Ramadhan, K., & Azhar, A. (2022). Design of PCF-SPR for Early Detection of Skin Cancer Infected Cells. *Jurnal Penelitian Pendidikan IPA*, *8*(5), 2293–2298. https://doi.org/10.29303/jppipa.v8i5.2120

disadvantages (Yan et al., 2021; Mahfuz et al., 2019; Danlard et al., 2022).

In determining the effect of each parameter on the PCF-SPR, several researchers have reported their findings, Yasli reported the effect of the PCF-SPR geometric structure on sensor performance, the domain observed was a circular, square, and oval-shaped geometric structure, and it was found that PCF-SPR with a hole size of the circle has high performance compared to other types, in 2022 Yasli also reported the effect of the metal layer and analyte channel on PCF-SPR, it was found that metal plating directly affects sensor sensitivity, it was also found that high sensitivity is obtained when the metal layer and analyte are located well outside as well as in the PCF structure while low sensitivity is obtained when the metal and analyte layers are located only in the cladding. In 2019, Yasli et al reported that related to the effect of plasmonic materials on the performance of the PCF-SPR sensor, the plasmonic materials used were gold, bimetallic silver-gold, and silver-graphene. It was found that graphene and silver materials have a high sensitivity of 4000 nm/RIU (Yasli & Ademgil, 2019). In this study, we examine the effect of air hole diameter size on our proposed sensor to detect skin cancer-infected cells, then we also examine the effect of plasmonic material thickness on the performance of the proposed sensor.

Method

The finite element method (FEM) was used in this study, the first thing to do is to construct the geometrical structure of the PCF, to arrange the air holes around the core and the PCF cladding, after that to arrange the analyte location, the thickness of the layer of plasmonic material and the thickness of the PML. The diameter of the sensor core is 5.875 µm. The size of the air hole contained in the core is distinguished in size, where the air hole closest to the gold layer has the largest size, namely d3, while the hole size at the next level is d2, while the air hole closest to the core has a diameter of d1 with their respective values are d1 = 0.3 µm, d2 = 0.48 µm, d3 = 0.6 µm. The small size of the hole in the middle is intended to facilitate the excitation of surface plasmon polariton (SPP). In addition, this hole size will also cause lateral leakage. So that in the sensor design, the polarization can be adjusted in the middle and as desired (Liu et al., 2020).

The distance between air holes d1 and d2 is 3.57 µm, while the distance between air holes d2 and d3 is 5.1 µm. This distance is based on the center of the hole to the center of the hole. This sensor design is also coated with gold plasmonic material with a thickness of 45 nm as shown in Figure 1, then in this paper will also be carried out variations of the effect of gold thickness to optimize sensor performance. The thickness of the analyte section is set to 0.5 µm, the gold layer is right after the core layer, followed by the analyte layer and the last layer of this sensor is PML to concentrate electromagnetic waves at the center of the sensor and there is no wave leakage, PML has a thickness of 1 µm.

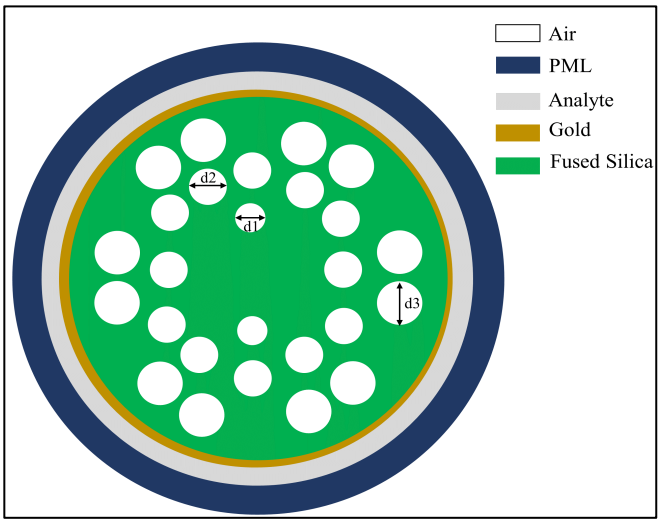

Figure 1. Geometry structure of the PCF-SPR sensor

In this paper, we investigate the PCF-SPR design using the finite element method (FEM) using COMSOL Multiphysics. In this investigation, PCF uses fused silica which can be defined by the sellmeier equation as in equation 1. Fused silica is the most commonly used PCF material, and is reported to have the best performance when compared to other materials such as TOPAS, Zeonex, etc. The sellmeier equation can be used in defining the fused silica material in the S-PCF-SPR design. The distribution of the refractive index for silica materials can be seen in Equation 1 (Rifat et al., 2016).

$$n(\lambda)=\sqrt{1+\frac{0.696\lambda^2}{\lambda^2-0.0047}+\frac{0.408\lambda^2}{\lambda^2-0.014}+\frac{0.897\lambda^2}{\lambda^2-97.934}} \quad (1)$$

Where n is the refractive index of silica for each particular wavelength, λ is the wavelength that illuminates the surface of the S-PCF-SPR. Plasmonic material is used to elicit the SPR effect on PCF, the plasmonic material used in this study is gold, gold is chemically more stable than the environment but shows a wide resonance peak and this will harm the components. The drude-Lorentz model is used in calculating the dielectric constant of gold which can be shown in Equation 2.

$$\varepsilon_{au}=\varepsilon_{\infty}-\frac{\omega_D^2}{\omega(\omega+j\gamma_D)}-\frac{\Delta\varepsilon\Omega_L^2}{\left(\omega^2-\Omega_L^2\right)+j\Gamma_L\omega} \quad (2)$$

With Au being the gold permittivity value, and high-frequency permittivity with a value of 5.9673, then is the plasma frequency, where D is the dumping frequency

and D is the plasmon frequency which numerically has a value of 31.84π THz and 4227.2π THz and the oscillator power with symbol L = 1300.14π THz, and the spectral width is L = 209.72π THz. PCF that has air holes around the surface will cause loss when I pass through the surface. This confinement loss can be defined as Equation 3.

$$L_c\left(dB/cm\right)=\left(\frac{4\pi f}{c}\right)\mathrm{Im}\left(n_{eff}\right)\times 10^4 \quad (3)$$

Where Lc is the material confinement loss, with a value of 3.14, f = frequency, neff is the effective refractive index, and c is the speed of light. Meanwhile, PCF-SPR performance factors such as wavelength sensitivity can be defined in Equation 4.

$$S_\lambda\left(nm/RIU\right)=\Delta\lambda_{peak}/\Delta n \quad (4)$$

Wavelength sensitivity shows how big the shift in the wavelength of the peak loss is for each change in the analyte's refractive index. A large shift for a small change in the refractive index of the analyte will show components that are ultra-sensitive and have high performance in distinguishing changes in the refractive index of the analyte. Wavelength sensitivity also shows the difference in peak loss at a certain wavelength divided by the difference in the sensing refractive index.

Table 1: Refractive index of infected cells and healthy cells causing cancer

Cancer	RI (Healthy)	RI (Infected)	Ref.
Skin	1.36	1.38	(Tsai, 2012)(Yaroslavsky et al., 2012)

Result and Discussion

The investigation carried out on the design of the PCF-SPR sensor is the FEM method. This method is effective and accurate in characterizing sensor performance, with the help of COMSOL simulation time will be faster. The sensor design that we propose has a real part relationship between refractive index and confinement loss which is shown in Figure 2. The sensor loss confinement is obtained from the imaginary value of the sensor's effective refractive index. to calculate the confinement loss follow equation 3. Each sensor geometry structure has various confinement loss values, this value depends on hole size, hole shape, the distance between holes, plasmonic material, and PCF dielectric material. In this proposed sensor design, we use a fused silica dielectric material which can be defined based on the Sellmeier equation in equation 1. Furthermore, gold is used as a plasmonic material whose dielectric constant can be defined following the Drude-Lorentz equation in equation 2.

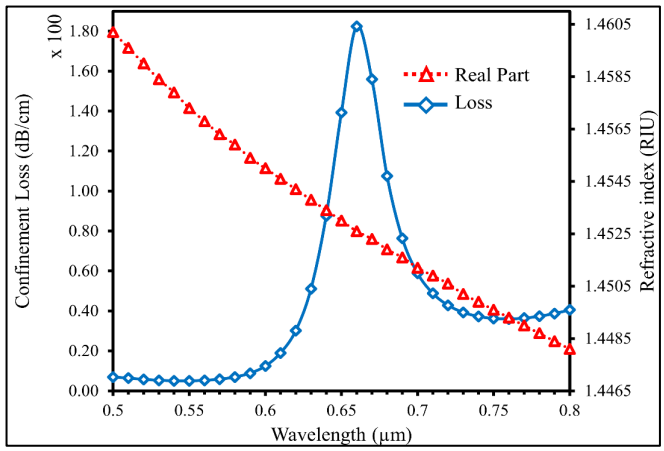

Figure 2. Real relation of refractive index vs confinement loss

According to Figure 2, we can see the relationship between the confinement loss and the real refractive index of the proposed sensor. The peak of the confinement loss is called the resonant wavelength of the PCF-SPR sensor. Resonance wavelengths arise due to plasmon resonance events around the gold surface. When light strikes a plasmonic material, an electron oscillation event will occur and this event is used to detect changes in the environment. Because it is very sensitive to environmental changes. When light passes through the fiber surface, there will be polarization around the 2D PCF surface. Polarization on the x and y axes can be seen in Figure 3(a) and Figure 3(b).

In this section, the effect of the size of the air hole in the form of a circle is tested on the performance of the PCF-SPR sensor. Figure 4. Figure 4(a) shows the confinement loss relationship obtained from y polarization with different hole sizes. The hole variations performed in this section are 1.1 μm, 1.2 μm, 1.3 μm, and 1.4 μm. It is found that the large air hole size has a small confinement loss value. At air holes with diameters of.1 m, 1.2 m, 1.3 m, and 1.4 m, respectively, the confinement loss peaks are 2017.21 dB/cm, 439 dB/cm, 72.9 dB/cm, 8.41 dB/cm. It is found that the larger the diameter of the air hole, the smaller the confinement loss on the proposed sensor. Meanwhile, the resonance wavelength of each air hole size shows the same value at 660 nm. There is no effect of hole size on the resonance wavelength in the proposed sensor (Wu et al., 2017).

Furthermore, in Figure 4(b) the confinement loss relationship obtained from the x polarization to the size of the air hole diameter in the proposed sensor geometry structure is obtained. The polarization of x also shows the same relationship between the size of the air hole diameter and the confinement loss sensor. In variations in diameter of 1.1 m, 1.2 m, 1.3 m, and 1.4 m, the

confinement loss peaks for each air hole diameter are 866.54 dB/cm, 182.41 dB/cm, 29.48 dB/cm, and 3.34 dB/cm. resonance wavelength has been found to be at 660 nm. The difference between the x and y polarizations is the peak value of the confinement loss. Polarization x has a confinement loss value that is smaller than the confinement loss on y (Rakibul Islam et al., 2020).

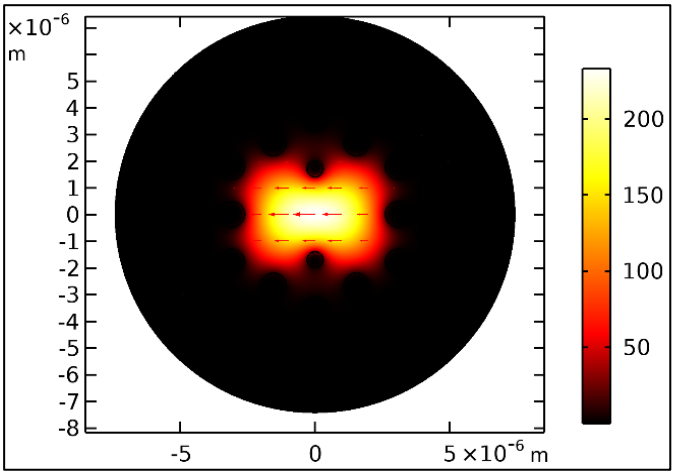

(a)

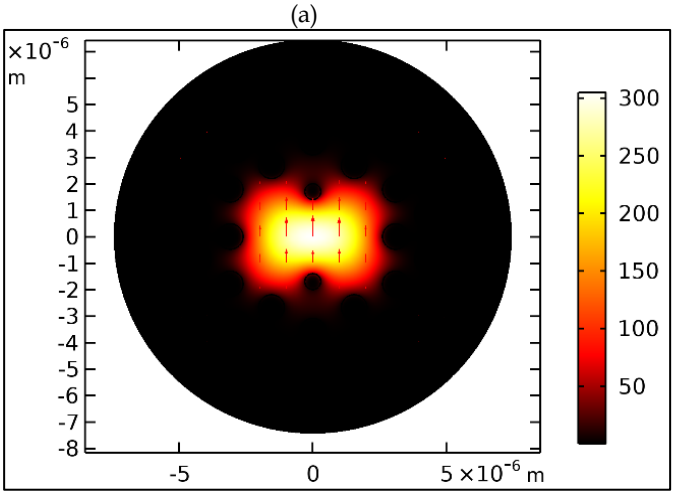

(b)

Figure 3. Polarization on PCF surface (a) x polarization, (b) y polarization

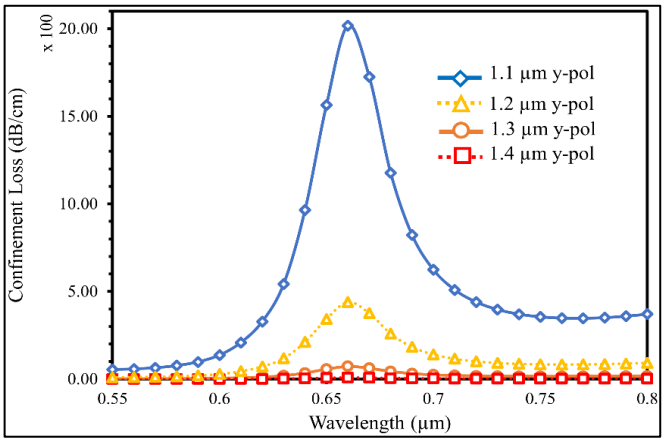

(a)

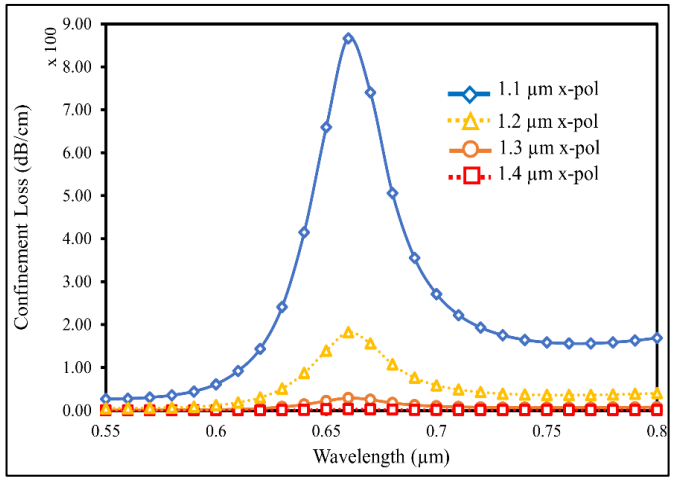

(b)

Figure 4. Effect of confinement loss on PCF-SPR air hole size (a) y polarization, (b) x polarization

Effect of the thickness of the plasmonic material on the performance of the proposed sensor

In this section, we discuss the effect of the thickness of the plasmonic material on the confinement loss sensor. in figure 5 we show the relationship obtained from our proposed sensor. Au thickness ranges from 40 nm, 45 nm and 50 nm. It was found that the proposed sensor has y polarization and x polarization. the polarization value is obtained that the y-axis has a greater value than the x-axis polarization. In the proposed sensor design, it is found that the confinement loss peaks on the sensor with gold kettle are 40 nm, 45 nm and 50 nm. They were obtained at 3.91 dB/cm, 3.34 dB/cm and 2.63 dB/cm in the x-axis polarization, with resonance wavelengths at 650 nm, 660 nm and 670 nm, respectively. There is a shift in the resonance wavelength as the thickness of the proposed sensor increases. The resonance wavelength shows the same value for the y-polarization, but what is significantly different is the confinement loss value (Mo et al., 2021).

In this design, it was found that the confinement loss of each thickness of gold on the y-axis polarization with variations in thickness of 40 nm, 45 nm, and 50 nm. They are 9.85 dB/cm, 8.4 dB/cm and 6.62 dB/cm, respectively. The thicker the gold layer indicates that the design confinement loss value is getting smaller, this happens because light cannot penetrate the thick gold layer on the PCF-SPR. This was also confirmed by many researchers in their study as reported by Sakib et al, they varied the thickness of the gold layer in the range of 30 nm, 40 nm and 50 nm. Confinement loss at 50 nm gold thickness has a small confinement loss value (Sakib et al., 2021), the same results have also been reported by Rahman et al, with variations in gold thickness of 25 nm, 30 nm, 40 nm, and 50 nm. that the thicker the gold layer the smaller the confinement loss value (M. T. Rahman et al., 2021).

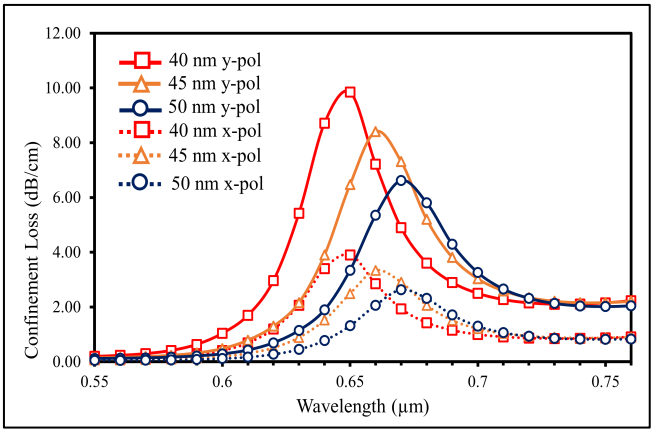

Figure 5. Effect of gold thickness on the performance of the proposed sensor

PCF-SPR sensitivity in detecting skin cancer cells

In this section, we carry out a sensitivity test on the proposed sensor design, using equation 4. We report that the proposed sensor has a wavelength sensitivity of 7000 nm/RIU in detecting skin cancer-infected cells and healthy cells. The resonance wavelength shift is shown in Figure 6.

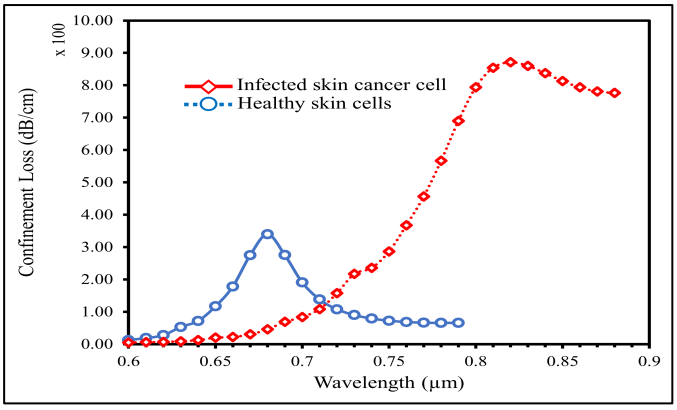

Figure 6. Resonance wave length shift in the proposed sensor

The resonance wavelength in detecting healthy cells is at 680 nm with a confinement loss value of 339.83 dB/cm, while in cells infected with skin cancer it is at 820 nm with a confinement loss value of 871.16 dB/cm, this result is better than previously reported by Yasli, his sensor proposed only has a wavelength sensitivity of 3150 nm/RIU (Yasli, 2021).

Conclusion

A numerical investigation has been carried out on the design of the PCF-SPR sensor using the COMSOL Multiphysics-based FEM method. PCF is defined as a fused silica material with the plasmonic material used in this investigation is gold. It was found that PCF-SPR has a wavelength sensitivity in detecting skin cancer-infected cells and healthy cells of 7000 nm/RIU, it is also found that the large hole diameter relationship results in a small confinement loss of the proposed PCF-SPR sensor. While the size of the thickness of the large plasmonic material gives a small confinement loss value. From the results of this numerical investment, it is recommended that the PCF-SPR sensor has good performance in detecting skin cancer cells.

Acknowledgements

We would like to thank LPPM Universitas Riau for their great support in this research under DRTPM Desentralisasi with contract no. 1643/UN19.5.1.3/PT.01.03/2022. We also would like to thank Optics and Optoelectronics laboratory and plasma and photonics physics laboratory.

References

Abdullah-Al-Shafi, M., & Sen, S. (2020). Design and analysis of a chemical sensing octagonal photonic crystal fiber (O-PCF) based optical sensor with high relative sensitivity for terahertz (THz) regime. *Sensing and Bio-Sensing Research*, *29*. https://doi.org/10.1016/j.sbsr.2020.100372

Danlard, I., Mensah, I. O., & Akowuah, E. K. (2022). Design and numerical analysis of a fractal cladding PCF-based plasmonic sensor for refractive index, temperature, and magnetic field. *Optik*, *258*. https://doi.org/10.1016/j.ijleo.2022.168893

Dash, J. N., & Jha, R. (2016). Highly Sensitive Side-Polished Birefringent PCF-Based SPR Sensor in near IR. *Plasmonics*, *11*(6), 1505–1509. https://doi.org/10.1007/s11468-016-0203-8

Irawan, D., Azhar, A., & Ramadhan, K. (2022). High-Performance Compensation Dispersion with Apodization Chirped Fiber Bragg Grating for Fiber Communication System. *Jurnal Penelitian Pendidikan IPA*, *8*(2), 992–999. https://doi.org/10.29303/jppipa.v8i2.1521

Irawan, D., Ramadhan, K., Saktioto, S., Fitmawati, F., Hanto, D., & Widiyatmoko, B. (2022a). Hexagonal two layers-photonics crystal fiber based on surface plasmon resonance with gold coating biosensor easy to fabricate. *Indonesian Journal of Electrical Engineering and Computer Science*, *28*(1), 146. https://doi.org/10.11591/ijeecs.v28.i1.pp146-154

Irawan, D., Ramadhan, K., Saktioto, S., & Marwin, A. (2022). Performance comparison of Topas chirped fiber bragg grating sensor with tanh and gaussian apodization. *Indonesian Journal of Electrical Engineering and Computer Science*, *26*(3), 1477–1485. https://doi.org/10.11591/ijeecs.v26.i3.pp1477-1485

Irawan, D., Ramadhan, K., Saktioto, T., Fitmawati, F., Hanto, D., & Widiyatmoko, B. (2022b). High-Performance of Star-Photonics Crystal Fiber Based

on Surface Plasmon Resonance Sensor. *Indian Journal of Pure & Applied Physics*, *60*(9), 727–733. https://doi.org/https://doi.org/10.56042/ijpap.v60i9.64411

Irawan D, S. T. (2014). Drug Delivery System Model using Optical Tweezer Spin Control. *Journal of Biosensors & Bioelectronics*, *05*(03). https://doi.org/10.4172/2155-6210.1000159

Liu, Q., Ma, Z., Wu, Q., & Wang, W. (2020). The biochemical sensor based on liquid-core photonic crystal fiber filled with gold, silver and aluminum. *Optics and Laser Technology*, *130*. https://doi.org/10.1016/j.optlastec.2020.106363

Mahfuz, M. Al, Mollah, M. A., Momota, M. R., Paul, A. K., Masud, A., Akter, S., & Hasan, M. R. (2019). Highly sensitive photonic crystal fiber plasmonic biosensor: Design and analysis. *Optical Materials*, *90*, 315–321. https://doi.org/10.1016/j.optmat.2019.02.012

Mo, X., Lv, J., Liu, Q., Jiang, X., & Si, G. (2021). A magnetic field SPR sensor based on temperature self-reference. *Sensors*, *21*(18). https://doi.org/10.3390/s21186130

Mollah, M. A., Yousufali, M., Ankan, I. M., Rahman, M. M., Sarker, H., & Chakrabarti, K. (2020). Twin core photonic crystal fiber refractive index sensor for early detection of blood cancer. *Sensing and Bio-Sensing Research*, *29*. https://doi.org/10.1016/j.sbsr.2020.100344

Rahman, K. M. M., Alam, M. S., & Islam, M. A. (2021). Highly Sensitive Surface Plasmon Resonance Refractive Index Multi-Channel Sensor for Multi-Analyte Sensing. *IEEE Sensors Journal*, *21*(24), 27422–27432. https://doi.org/10.1109/JSEN.2021.3126624

Rahman, M. T., Datto, S., & Sakib, M. N. (2021). Highly sensitive circular slotted gold-coated micro channel photonic crystal fiber based plasmonic biosensor. *OSA Continuum*, *4*(6), 1808. https://doi.org/10.1364/osac.425279

Rakibul Islam, M., Iftekher, A. N. M., Rakibul Hasan, K., Nayen, M. J., & Bin Islam, S. (2020). Dual-polarized highly sensitive surface-plasmon-resonance-based chemical and biomolecular sensor. *Applied Optics*, *59*(11), 3296. https://doi.org/10.1364/ao.383352

Ramadhan, K. (2020). Dispersi multi-layer pada inti serat optik moda tunggal. *Seminar Nasional Fisika Universitas Riau V (SNFUR-5)*, 1–5.

Ramadhan, K., & Saktioto, T. (2021). Integrasi Chirping dan Apodisasi Bahan TOPAS untuk Peningkatan Kinerja Sensor Serat Kisi Bragg. *Komunikasi Fisika Indonesia*, *18*(2), 111–123. https://doi.org/http://dx.doi.org/10.31258/jkfi.18.2.111-123

Ramola, A., Marwaha, A., & Singh, S. (2021). Design and investigation of a dedicated PCF SPR biosensor for CANCER exposure employing external sensing. *Applied Physics A: Materials Science and Processing*, *127*(9). https://doi.org/10.1007/s00339-021-04785-2

Rifat, A. A., Mahdiraji, G. A., Ahmed, R., Chow, D. M., Sua, Y. M., Shee, Y. G., & Adikan, F. R. M. (2016). Copper-graphene-based photonic crystal fiber plasmonic biosensor. *IEEE Photonics Journal*, *8*(1). https://doi.org/10.1109/JPHOT.2015.2510632

Sakib, N., Hassan, W., & Rahman, T. (2021). Performance study of a highly sensitive plasmonic sensor based on microstructure photonics using an outside detecting method. *OSA Continuum*, *4*(10), 2615. https://doi.org/10.1364/osac.433758

Saktioto, T., Ramadhan, K., Soerbakti, Y., Irawan, D., & Okfalisa. (2021a). Apodization sensor performance for TOPAS fiber Bragg grating. *Telkomnika*, *19*(6). https://doi.org/http://dx.doi.org/10.12928/telkomnika.v19i6.21669

Saktioto, T., Ramadhan, K., Soerbakti, Y., Irawan, D., & Okfalisa. (2021b). Integration of chirping and apodization of Topas materials for improving the performance of fiber Bragg grating sensors. *Journal of Physics: Conference Series*, *2049*(1). https://doi.org/10.1088/1742-6596/2049/1/012001

Tsai, C. C. (2012). *Water distribution in cancer and normal cells*.

Wu, T., Shao, Y., Wang, Y., Cao, S., Cao, W., Zhang, F., Liao, C., He, J., Huang, Y., Hou, M., & Wang, Y. (2017). Surface plasmon resonance biosensor based on gold-coated side-polished hexagonal structure photonic crystal fiber. *Optics Express*, *25*(17), 20313. https://doi.org/10.1364/oe.25.020313

Yan, X., Wang, Y., Cheng, T., & Li, S. (2021). Photonic crystal fiber spr liquid sensor based on elliptical detective channel. *Micromachines*, *12*(4). https://doi.org/10.3390/mi12040408

Yaroslavsky, A. N., Patel, R., Salomatina, E., Li, C., Lin, C., Al-Arashi, M., & Neel, V. (2012). High-contrast mapping of basal cell carcinomas. *Optics Letters*, *37*(4), 644. https://doi.org/10.1364/ol.37.000644

Yasli, A. (2021). Cancer Detection with Surface Plasmon Resonance-Based Photonic Crystal Fiber Biosensor. *Plasmonics*, *16*(5), 1605–1612. https://doi.org/10.1007/s11468-021-01425-6

Yasli, A., & Ademgil, H. (2019). Effect of plasmonic materials on photonic crystal fiber based surface plasmon resonance sensors. *Modern Physics Letters B*, *33*(13). https://doi.org/10.1142/S0217984919501574